SSRG International Journal of Material Science and Engineering
ISSN: 2394–8884 / https://doi.org/10.14445/23948884/IJMSE-V12I1P102

Volume 12 Issue 1, 8-23, Jan-Apr 2026

Original Article

Effect of Eggshell Particles on Mechanical Properties of Recycled Aluminium Beverage Cans

Victor O. Hammed[1], Taopheeck T. Yusuf[2], Abdulrahman M. Hassan[3], Azeez A. Bankole[4], Ibitoye S. Ademola[5]

[1,2,3,4,5]*Department of Materials Science and Engineering, Obafemi Awolowo University, Ile-Ife. Nigeria.*

[1]*Corresponding Author : hammedvictor@gmail.com*

Received: 17 February 2026 Revised: 22 March 2026 Accepted: 10 April 2026 Published: 28 April 2026

Abstract *- The study investigated the effect of pulverized Eggshell (ES) particles on the mechanical properties of recycled aluminium beverage cans. This involved melting and alloying aluminium beverage cans with ES particles at weight percentages [2% - 10%], at intervals of 2%, and casting the alloyed aluminium into cylindrical rods of 200 mm X 20 mm. Subsequently, this was machined into standard test specimens for testing tensile strength, hardness, and impact strength. Elemental and microstructural compositional analyses were also conducted. Results showed a tensile strength of 108 MPa for the control sample. This decreased with additional 2 wt%, 4 wt%, and 6 wt% eggshell particles, but increased with 8 wt% and 10 wt% additions, achieving a maximum of 133 MPa at 8 wt%. The values of Brinell hardness increased slightly with 2 wt% and 4 wt% ES, but showed a sharp decline at 6 wt%. It increased significantly with 8 wt% and 10 wt% ES. Inversely, impact strength values decreased with increasing eggshell content. The study concluded that ES particles, primarily composed of calcium, combined with aluminium to form an intermetallic compound known as Al4Ca, are effective as a grain refiner when ES content is between 8-10 wt%. Thus, hardness and tensile strength are improved while minimising impact toughness.*

Keywords *- Recycling, Eggshell, Aluminium Beverage Cans, Environmental Sustainability.*

1. Introduction

1.1. Global Context

The aluminium industry is one of the most important sectors in global manufacturing. Global production of primary aluminium exceeded 50 million metric tons in 2019, with beverage cans accounting for up to 15% of total aluminium consumption (Kolbeinsen, 2020).

Specifically, the beverage can market produces approximately 400 billion aluminum cans annually, with recycling rates of 74-78% in Europe and 65-75% in North America, respectively (Dudubo, 2017). This scale, with reference to global implications, underscores the economic opportunity inherent in and environmental imperative of enhancing the properties of recycled aluminium.

Aluminium and aluminium alloys are indispensable materials in modern manufacturing. This is as a result of their characteristic properties, including high strength-to-weight ratio, low density, superior thermal and electrical conductivity, and excellent corrosion resistance (Mohanavel et al., 2020). The beverage can industry is one of the largest consumers of aluminium. Billions of cans are produced annually worldwide (Sapotal, 2019). Specifically, the typical aluminium-based beverage can is produced from the AA3004 and AA5182 alloys, respectively for the body and the lid, and both are optimized for strength and formability (Juniarsih, Oediyani, & Zain, 2019).

1.2. Economic and Environmental Imperative

Aluminium recycling also produces substantial energy savings, with the production of recycled aluminium requiring 5% of the energy required for primary production. This translates to energy savings of up to 14,000 kWh/ton of recycled material.

In turn, this reduction in energy corresponds to a reduction in carbon footprint of up to 9 tons of CO_2, equivalent per ton of recycled aluminum instead of that produced from bauxite ore (Gautam, Pandey, & Agrawal, 2018). With reference to global recycling volumes, this makes up to 100 million tons equivalent of annual CO_2 emission reduction.

Similarly, Eggshell (ES) particles have compelling economic implications. With the global aluminium recycling market valued at $42.4 billion, and projections indicating sustained growth powered by sustainability regulations and circular economy initiatives (Shashikala, 2020), recycling aluminium cans also saves up to $80-$1000/ton compared to primary costs of production, which fails to account for the environmental externalities not taken into consideration.

1.3. Eggshell Waste as an Environmental Challenge

Furthermore, Eggshell (ES) particles waste produces an environmental challenge, with global egg production generating up to 547,000 tons annually. Eggshells primarily consist of calcium carbonate, trace minerals, and organic matrix proteins (Quina, Soares, & Quinta-Ferreira, 2017). From recent research, studies have demonstrated the potential of using food industry and agricultural wastes as sustainable reinforcement materials, and incorporating eggshell particles into the metal matrix composites offers the benefit of material property enhancement and waste valorization (Dwivedi, Sharma, & Mishra, 2017), by refining the grains and fostering strengthening methods. The majority of this waste is currently being disposed of in landfills or incinerated, which represents an extinct resource opportunity and a waste management concern.

Meanwhile, merging the two waste streams: the eggshells and aluminium beverage cans, presents an opportunity for waste valorization, where the two environmental challenges will be addressed while creating superior recycled materials (Garcia-Chevesich et al., 2020). This aligns with the United Nations Sustainable Development Goal 12 (Responsible Consumption and Production) and the circular economy framework recommended by organizations worldwide (Chan et al., 2018).

1.4. The Problem of Technical Degradation

Recycling aluminium beverage cans provides substantial economic and environmental benefits as the process requires only 15% of the energy required to produce primary aluminium, hence, reducing carbon emissions and resource wastage or depletion (Niero & Olsen, 2016; Stotz et al., 2017). However, one challenge persists, which is the continuous exposure of aluminium to degradation in mechanical properties primarily as a result of microstructural coarsening and contamination during repeated melting (Summers et al., 2015). Therefore, cost-effective reinforcement strategies must be developed to restore or improve the properties of recycled aluminium.

Repeated thermal cycling can modify precipitate size and distribution, especially affecting strengthening phases in alloys (Sun et al., 2019). Likewise, progressive accumulation of silicon, iron, and other elements from contamination sources leads to brittle, hard intermetallic phases, which reduce ductility (Ebhota & Jen, 2018).

During melting, prolonged exposure to high temperatures can promote grain growth by migrating thermally-activated boundaries, minimizing grain boundary area, and reducing strength through the Hall-Petch relationship (Chokshi, 2020).

Overall, recycled aluminium faces degradation challenges, where each melting cycle introduces effects ranging from an increase in grain size due to grain coarsening to a reduction in tensile strength and a decline in ductility for each recycling iteration.

1.5. Current Solutions and Limitations

Against the backdrop, there is a need for cost-effective and environmentally sustainable alternatives capable of restoring or enhancing mechanical properties and maintaining the recycling operations' economic viability (Ribeiro et al., 2016). According to Soo et al. (2018), blended recycled material with at least 20% virgin aluminium restores the material's properties, while undermining the environmental benefits and increasing costs. Similarly, commercial Al-Ti-B alloys help to refine the grain structure. However, they are costly and economically unreasonable for various recycling operations (Fan et al., 2015). Moreover, contamination can be minimized through sophisticated separation technologies, but this can only be achieved by investing a substantive amount in the facility, up to $2-5 million/facility, although critics argue that this does not help to address grain coarsening.

1.6. Research Significance

This research addresses these gaps by contributing different dimensions of insights. First, the simultaneous use of two waste streams of aluminium cans and eggshells represents an innovative circular economy approach that is not fully captured in existing literature. Second, ES particles are highly cost-effective, particularly since they cost nothing compared to other grain refiners. This helps to significantly reduce the costs of reinforcement.

Third, although the grain refining capacity of calcium is known, eggshell-derived calcium in recycled beverage can alloys, that is AA3004/AA5182, is under-investigated. In addition, the 8-10 wt% range for optimal property enhancement offers actionable guidance for industrial applications. Again, the processing methods used, which involve stir casting at compatible parameters with existing foundry equipment, drive potential industrial applications without the need for specialized infrastructure.

2. Literature Review

2.1. Recycling: Aluminium Beverage Cans

Since its introduction in the 1950s, the aluminium beverage can has evolved remarkably. In modern times, a two-piece design produced via deep drawing and wall ironing processes is used to produce beverage cans (Borah & Dutta, 2019). The body, made of AA3004 alloy, contains at least 1.0% manganese, 0.8% magnesium, and controlled silicon and iron, contributing to improved strength and formability. The lid, made of AA5182 alloy, contains magnesium (4.0 – 5.0%) for improved retention properties and strength (Mutsakatira, 2020).

According to Capuzzi & Timelli (2018), aluminium recycling is a circular economy idea, involving the collection, shredding, de-coating, melting, and casting. Repeated

recycling, however, results in accumulated impurities, grain coarsening, and degradation of the material's properties. Strategic alloying using bio-derived materials can potentially counteract these effects and promote environmental sustainability (Dodson et al., 2015; Marques et al., 2020).

2.1.1. Microstructural Evolution at Recycling

The knowledge of degradation mechanisms demands that microstructural changes be examined across recycling cycles. During recycling, grain growth follows the kinetics described by $d2 - d02 = kt$, where d is the grain size, t is time at temperature, and k is a temperature-based constant (Doan-Nguyen, 2015). Grain growth rates of 15-30μm per hour are common for aluminium alloys at melting temperatures of 700 – 750 ° C. This results in grain sizes exceeding 150 μm after several cycles without introducing grain refining techniques (Hidalgo & Santofimia, 2016).

Likewise, phase transformation occurs in AA3004 alloys, where dispersoids containing manganese can coarsen up to 500 nm due to repeated cycling, which consequently reduces their strengthening ability. In addition, magnesium-rich beta-phase (Mg_2Si) particles in AA5182 alloys undergo Ostwald ripening, in which larger particles outgrow smaller ones, thereby increasing the strength of precipitation (van Westen & Groot, 2018).

2.1.2. Effects and Pathways of Contamination

Impurity accumulation is a major degradation factor. Due to processing equipment and ferrous metal cross-contamination, iron contamination accumulates at 0.02 – 0.05 wt% per recycling cycle (Brooks et al., 2019). Similarly, silicon accumulates from paint coatings and contamination. Although moderate silicon levels of 0.4 – 0.8 wt% can enhance fluidity, excessive concentrations encourage the formation of irregular and hard Si particles, which can take a toll on mechanical properties (Hauksdottir, 2016). Other contaminants, such as copper, zinc, and tin from mixed scrap sources, affect alloy performance through various mechanisms.

2.1.3. Economic and Regulatory Drivers

Regulatory frameworks are effective for incentivizing recycling optimization. By 2030, the European Union's Circular Economy Action Plan mandates that the recycling rate targets should be up to 85% for aluminum packaging. Also, Extended Producer Responsibility (EPR) policies in more than 35 countries create economic incentives for improving the quality of recycled material. Through these regulations, a market pull is created for technologies that can enhance the properties of recycled aluminum.

Moreover, these drivers are amplified by the market demand for sustainable materials. Specifically, corporate commitments towards sustainability, including commitments by major beverage-producing companies to increase recycled content to 50-75% by 2030, create a huge demand for quality recycled aluminium (Soo et al., 2018).

2.2. Analysis of Bio-Waste Reinforcements

Bio-waste reinforcements for aluminium composites go beyond eggshells. First, Rice Husk Ash (RHA), which contains 85-90% amorphous silica, has demonstrated promising results in Al-Si alloys, where 6-10 wt% additions improve hardness (Hossain & Roy, 2020). However, the silica content of the material makes it unsuitable for non-silicon-containing aluminium alloys. When added at a certain weighted percentage, coconut shell char particles help to improve wear resistance via carbon enrichment at the surface, but with little strength enhancement (Bello, 2017). Similarly, studies have explored bamboo fiber reinforcement, where 2-6 wt% additions increase tensile strength by approximately 15%, yet they introduce processing challenges due to high thermal degradation (Ain et al., 2016).

Conversely, eggshell particles are beneficial for their widespread availability in all geographic regions, simple processing, requiring calcination and grinding (Waheed et al., 2020), thermal stability to facilitate processing at aluminium melting temperatures without degradation, and calcium content for characteristic grain refining capability in carbon- or silica-based reinforcements (Gao et al., 2020).

Many studies have examined the potential use of eggshell particles in reinforcing aluminium matrix composites. According to Agunsoye et al. (2015), recycled aluminium cans and Eggshell (ES) composites can help improve wear resistance and mechanical properties of the materials. When processed and distributed well, ES particles can enhance the tribological performance and strength of recycled aluminium (Hayajneh, Almomani, & Al-Shrida, 2019).

Likewise, in a study examining the mechanical properties and microstructures of Al-Si-Mg-Ti/eggshell particulate composites, ES particle additions up to certain weight percentages (wt%) showed a clear improvement in hardness and tensile strength (Shamim et al., 2017). These improvements are attributed to the effects of grain refinement and calcium-rich intermetallic phases. Furthermore, the particle size and distribution of the mechanical and microstructural properties of ES-reinforced AI6061 alloy can influence the consequent composite properties (Dwiwedi et al., 2018).

Moreover, Dwivedi, Sharma, and Mishra's research (2017) on eggshell-based composite materials found that the range of optimal reinforcement levels is between 4-12 wt%, where peak properties are achieved at corresponding intermediate additions. Generally, eggshell particles act as sources of calcium and reinforcement for intermetallic formation (Hayajneh et al., 2019).

2.3. Phase Equilibria of Calcium-Aluminum

The binary phase diagram of Al-Ca reveals limited calcium in aluminum solubility, with a maximum of 0.05 wt% at 616°C, leading to intermetallic formation. There are four primary intermetallic phases, namely Al4Ca, Al2Ca, Al3Ca8, and Al14Ca13 (Akopyan, Belov, & Naumova, 2018). The sequence of phase formation during solidification depends on the concentration of calcium, especially as less than 5 wt% Ca causes primary aluminium to solidify first, and Al4Ca's formation afterward. On the other hand, above 7 wt% Ca, primary Al4Ca precipitates from the melt, giving more effective grain refinement by increasing the potential for nucleation (Belov, Naumova, & Akopyan, 2015).

However, the binary picture is complicated by ternary effects. Essentially, magnesium at 4-5 wt% in AA5182 alloys interacts with calcium to produce (Al, Mg)2Ca phases that alter solidification behavior and mechanical properties. Similarly, silicon influences phase selection, where Al2Si2Ca ternary phases are formed in high-silicon alloys.

2.4. Grain Refinement of Calcium-Aluminium Intermetallic Compounds

The calcium-aluminium interaction leads to the formation of different intermetallic compounds: Al_2Ca, Al_4Ca, $Al_{14}Ca_{13}$, and Al_3Ca_8. Al4Ca is typically effective for grain refinement in Al alloys (Guan & Tie, 2017). For instance, research on grain refinement approaches highlights that high-melting-point calcium-based intermetallic phases, such as Al4Ca and CaAl2, are heterogeneous nucleation sites during solidification (Li et al., 2017).

In addition, Zhang et al. (2017) demonstrated that in grain refinement of aluminium alloys, different mechanisms such as heterogenous nucleation and constitutional supercooling are involved. Calcium-based compounds facilitate grain refinement through these two mechanisms, where the calcium atoms segregate to grain boundaries at solidification, and increase constitutional supercooling (StJohn et al., 2015; Greer, 2016), while calcium-based particles are nucleation sites for alpha-aluminium grains.

Research on Al-Mg-Si alloys and Al-Ti-B grain refiners established the role of grain refinement in improving mechanical properties by enhancing grain boundary area, which represents a barrier to dislocation movement and improves strength via the Hall-Petch relationship (Boyko, 2015). Calcium-induced grain refinement follows the same mechanisms as coarse columnar structures are replaced by fine equiaxed grains, to improve ductility and strength (Li et al., 2020).

The effectiveness of grain refinement depends on meeting the nucleation and growth restriction criteria. The heterogenous nucleation potential is demonstrated by the Free Growth Model, showing the potency of heterogenous nucleation expressed in $d_{grain} = a + b/Q$, where Q is the growth restriction factor, while a and b are constants (Bazhenov & Magura, 2018). For Ca in Aluminium, Q ~ 12-15 K, which indicates strong growth restriction compared to Q ~ 3-5K for traditional solutes like titanium.

Constitutional supercooling is described by $\Delta T_c = m_L C_0(1-k)/k \times G/R$, where m_L is the liquidus slope, k is the partition coefficient, G is the temperature gradient, R is the growth rate, and Co is the composition. The low solid solubility of calcium (k ~ 0.002) creates huge constitutional supercooling irrespective of its concentrations, which promotes nucleation prior to solidification (StJohn et al., 2015).

Particle potency is also critical. Al4Ca particles reveal crystallographic compatibility with aluminium via a low lattice mismatch of ~ 4-6%, which satisfies the <15% criterion for successful heterogeneous nucleation (Sauvage et al., 2020). The nucleation energy barrier is minimised through this structural similarity, and enables grain refinement at relatively moderate particle densities.

2.5. Science of Composite Manufacturing: Processing and Optimization Methods

The most widely used technique for fabricating metal matrix composites is stir casting, especially because it is cost-effective and relatively simple (Kandpal, Kumar, & Singh, 2018). Stir casting parameters were optimized for eggshell-reinforced aluminium composites, which identifies major process variables such as stirring speed (400-600 rpm), pouring temperature (700-750 degrees Celsius), and stirring time (10-15 minutes) (Arunkumar et al., 2020). This was based on the premise that properly selecting parameters ensures uniform distribution of the particles while minimizing porosity. Stir casting has complex fluid dynamics.

Particle entrainment efficiency is determined by the vortex formation, expressed in $Ri = (g\Delta\rho H)/(\rho U^2)$, where $\Delta\rho$ represents the density difference, g is gravitational acceleration, ρ is liquid density, H is liquid height, and U is stirring velocity (Abdul, 2019). Therefore, aluminium-eggshell systems that have a density mismatch of ~ 1.4 g/cm3, Ri of 0.3 – 0.8 (from 450-550 rpm) optimize particle capture and minimize air entrapment.

Yuan et al. (2018) wrote that particle size has a significant impact on composite materials. ES particles within the range of 150-250 μm provide reinforcement efficiency, with finer particles offering greater surface area for interfacial bonding, although they risk agglomeration. On the other hand, coarser particles minimise clustering while providing less effective strengthening (Wu et al., 2016). Calcination and other popular pre-treatment methods, involving heating to 500 – 900 degrees Celsius, remove organic components while enhancing particle-matrix compatibility (Singh, 2017).

In addition, wettability is largely affected by temperature control. Wetting improves with an increase in temperature, while the contact angle between calcium carbonate and molten aluminium decreases (Barandehfard et al., 2020). However, the practical processing window is limited by temperature exceeding 800 °C, due to excessive calcium vaporization and $CaCO_3$ decomposition (Wani et al., 2018).

2.6. Formation and Mitigation of Defects

Porosity in the metal matrix is attributed to entrapment of gas during stirring, making ~ 40% of total porosity, ~ 35% of hydrogen absorption from moisture in reinforcement particles, and ~ 25% solidification shrinkage (Etemadi et al., 2015). Pre-calcining eggshell reinforcements at high temperature for 2 hours removes moisture and organic content, and consequently cuts hydrogen-based porosity.

Moreover, kinetic and thermodynamic drivers produce particle clustering. Particles can concentrate in interdendritic regions when forces are pushed from solidification fronts, while agglomeration can be triggered by attractive Van der Waals forces, especially when the distance in particle separation decreases below ~500 nm (Wang & Shi, 2019). Likewise, electromagnetic stirring and ultrasonic treatment at solidification gives up to 30-50% reduction in cluster size through particle network disruption before the end of solidification.

2.7. Strengthening Mechanisms

Many strengthening mechanisms operate concurrently in particle-reinforced composites. Hall-Petch strengthening is demonstrated in the equation: $\sigma\_HP = \sigma_0 + k\_y\ d^{(-1/2)}$, where k_y is the Hall-Petch slope, σ_0 is the friction stress, and d is grain size (Armstrong, 2018). The strength increases up to 25-35 MPa by reducing the grain size from 100 μm to 40 μm. Also, in Orowan strengthening, described by $\Delta\sigma\_Orowan = 0.4MGb/\lambda\ ln(D/2b)$, M is the Taylor factor (~ 3.1 for FCC aluminium), b is Burger's vector (~ 0.286nm), λ represents interparticle spacing, D is particle diameter, and G is shear modulus (~ 26 GPa). This contributes additional strength for non-shearable particles (Liu et al., 2015; Barnett, Wang, & Guo, 2019). For instance, for Al4Ca particles with λ of ~ 8-12 μm, and D = ~ 2-5 μm, the alloy can be strengthened by 15-25 MPa.

Furthermore, particle aspect ratio and interfacial bonding determine the efficiency of load transfer, where the shear lag model predicts the effectiveness of load transfer scales with (L/D), where L represents particle length, and D represents the diameter. Studies show that load transfer contributes an average of 10% of the total strength of the composite in roughly equiaxed Al4Ca particles, where L/D ~ 1.2-1.8 (Poblete & Zhu, 2019).

Meanwhile, thermal mismatch strengthening usually occurs due to coefficient of thermal expansion (CTE) differences, as $\alpha\_Al \approx 23\times10^{-6}\ K^{-1}$ vs. $\alpha\_CaO \approx 12\times10^{-6}\ K^{-1}$ produces residual stresses while cooling, and generates dislocation densities of near particle-matrix interfaces (10 13 – 10 13 m-2) (Monroe et al., 2016).

2.8. Particle Size Optimization Theory

Selecting particle size involves several considerations, which often compete due to certain reasons. Finer particles of 50 – 100 μm can maximize surface area for interfacial bonding while reducing interparticle spacing, hence, enhancing Orowan strengthening. However, they have a higher agglomeration tendency and potentially create weak clustered regions (Arvaniti et al., 2015). On the other hand, coarser particles of (250-500 μm) resist clustering due to reduced surface energy, but provide less effective grain refinement as a result of reduced particle number density (where particle count scales as D-3 for constant weight fraction) (Davies, 2017). The optimum range is 150-250 μm, which balances the competing factors, particularly in aluminium matrix systems (Kumar & Venkatesh, 2019).

2.9. Interfacial Chemistry and Bonding

Composite integrity is governed by interfacial reactions. Calcium carbonate undergoes thermal decomposition at 700-750 °C temperatures, involving Arrhenius-kinetics based reaction rates with activation energy E_a ~ 200-220 kJ/mol (Ahmad, 2016). Consequently, calcium oxide reacts with molten aluminium in the equation $4Al + CaO = Al_4Ca + Al_2O_3$, which forms the anticipated intermetallic phase and alumina particles to further enhance strength by dispersion hardening (Adabifiroozjaei, 2017).

Interfacial bonding is affected by wetting behavior. In the Young-Dupre equation, $W\_ad = y\_LV\ (1 + \cos\theta)$, work of adhesion W_ad is related to liquid-vapor surface tension y_LV and contact angle θ. Therefore, for Al-CaO systems, contact angles decrease from 110 ° to 75 ° at 700-800 ° C, which indicates stronger bonding and improved wetting at higher temperatures (Ahmad et al., 2018).

Besides, reaction product morphology influences the composite's properties. For example, at ~ 50 -200 nm, continuous Al_2O_3 layers at particle-matrix interfaces improve load transfer via strong interfacial bonding, and thick (> 500 nm) or discontinuous layers lead to weak interfacial zones that are susceptible to debonding (Kaleemulla & Doddamani, 2019).

2.10. Research Gaps

Despite extensive research on this phenomenon, significant gaps persist. First, cyclic loading behavior is yet to be characterized, but presents a major requirement for the composite's structural applications. Second, there is limited data on the electrochemical behavior of ES-reinforced composites, especially in acidic beverage environments with a pH of 2-5-3.5, which is typical of soft drinks. Third, no

current studies have examined ES-reinforced recycled aluminium's property retention over several subsequent recycling cycles, which are critical for assessing the actual circular economy potential.

Fourth, the synergies between ES particles and other treatments or reinforcements, such as conventional grain refiners or heat treatment, are yet unexplored, with a corresponding lack of comprehensive life cycle cost analyses that compare ES reinforcement to conventional approaches.

Finally, most studies typically use laboratory-scale casting of 100g-2kg, implying that industrial validation at production scales, especially up to 1000kg, is lacking. Thus, this research addresses these gaps and acknowledges comprehensive characterization across multiple dimensions as a continuous research focus.

3. Methodology

3.1. Materials

Recycled aluminium beverage cans, which have approximately 90.5% Aluminium content, represent the matrix material. Fresh chicken eggshells, comprising approximately 95% $CaCO_3$, were collected locally, washed thoroughly, and sun-dried to remove organic membranes and moisture.

3.2. Sample Preparation

3.2.1. Preparing Eggshell

Dried eggshells (ES) were crushed and ground with a mechanical grinding machine, after which the resulting powder was sieved to achieve 150 μm-sized particles. This particle size was deemed suitable and selected based on recommendations from the literature regarding mechanical property enhancement and optimal dispersion.

Fig. 1 Eggshell [Collected from local sources]

Fig. 2 Sieved eggshell particles of 150 micron size

3.2.2. Processing can

Aluminium beverage cans were collected, cleaned, de-coated, and compressed with a hydraulic press to reduce volume and enhance melting.

Fig. 3 Aluminium beverage cans

3.2.3. Melting and Casting

Compressed cans were melted at 750 degrees Celsius in a crucible furnace. Upon complete melting and removal of slag, preheated ES particles (heated for 1 hour at 500 degrees Celsius) were added in various weight percentages (wt%): 0% (control), and 2% - 10% in 2% increments. The molten composite was stirred mechanically at 500 rpm for 10 minutes for uniform distribution of the particles. The composite melt was poured into cylindrical molds (200 mm by 20 mm) and preheated to 200 degrees Celsius. Each composition was prepared and labelled as Control (0% ES), 2% ES, 4% ES, 6% ES, 8% ES, and 10% ES.

Fig. 4 Melting compressed cans in a furnace

Fig. 5 Mixing and stirring of ES particles with the molten metal in the ladle

Fig. 6 Composite melt poured into cylindrical molds

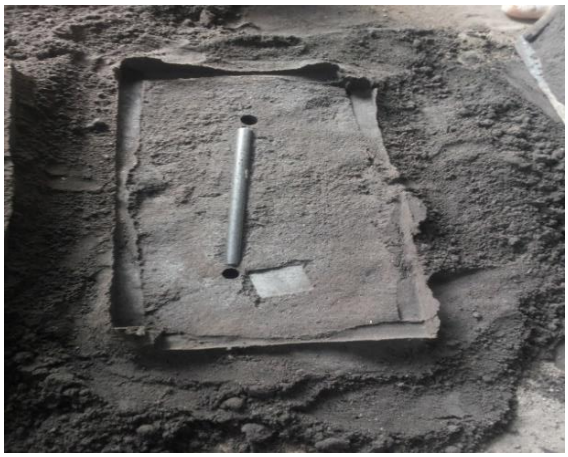

Fig. 7 Preparing samples

3.3. Characterization Procedures

3.3.1. Mechanical Testing

For mechanical testing, cast rods were machined into specimens, and tensile tests were performed using a universal testing machine at a speed of 2mm/min according to ASTM E8 standards. The specimens were also tested for hardness using the Brinell hardness, involving a 10 mm steel ball indenter with a 500 kg load for 30 seconds. A Charpy impact tester was used to conduct the impact tests. The specimens were notched per ASTM E23 standards.

Fig. 8 Mechanical testing of cast rods

Fig. 9 Cast rod specimens

3.3.2. Compositional Analysis

Particle-Induced X-ray Emission (PIXE) spectroscopy was performed to determine elemental composition and accurately quantify elements, including magnesium and other heavier elements in the periodic table.

3.3.3. Microstructural Analysis

Sample specimens for metallographic tests were prepared with the standard grinding process (240, 400, 600, 800, 1000 grit SiC papers) and polishing procedures. Etched samples comprising Keller's reagent of 2 ml HF, 3 ml HCl, 5 ml HNO3, and 190 ml H2) were examined with optical microscopy at 100 times magnification in order to identify grain structure and intermetallic distribution at different phases.

4. Results and Discussion

4.1. Tensile Properties

The control sample showed a tensile strength of 108 MPa and a yield strength of 52 MPa. Adding weighted percentage of ES in increments of 2 led to decreases in tensile strength of 95 MPa (at 2 wt%), 88 MPa (at 4 wt%), and 82 MPa (at 6 wt%). However, the study showed significant improvements with higher reinforcement levels: 8 wt% ES produced 133 MPa (23% higher than the control), and 10 wt% ES produced 125 MPa. Results on yield strength implied a progressive increase from 52 MPa to 78 MPa at 10 wt% ES.

Decreasing tensile strength at the start with low ES particle additions can be attributed to inadequate grain refinement and the introduction of porosity. Below a 6-8 wt% threshold, insufficient calcium is available for the effective formation of Al4Ca, while ES particles may be used as stress concentrators. This aligns with Parande et al.'s findings (2020), who identified that non-linear property variations exist in ES-reinforced composites.

The improvement at 8 wt% and above is due to the combined effects of strengthened precipitation and grain refinement. According to Jiang et al. (2016), calcium content above 7% leads to the formation of Al4Ca intermetallic compounds, acting as effective grain refiners. The refined grain structure increases the grain's boundary, constraining dislocation movement via the Hall-Petch strengthening procedure. In addition, fine Al4Ca precipitates are distributed within the matrix, giving Orowan strengthening which forces particle-based dislocations (Thompson et al., 2018).

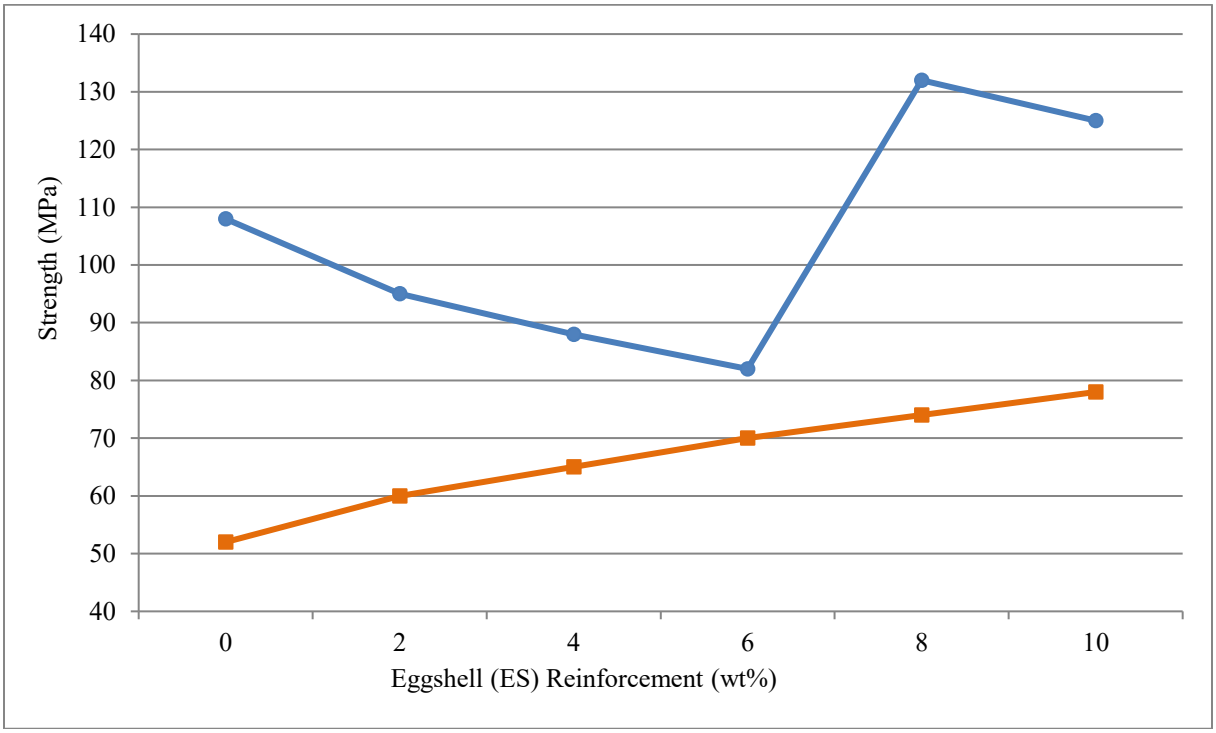

Fig. 10 Illustrative relationship between Eggshell (ES) reinforcement percentage and both tensile and yield strengths

4.2. Hardness Properties

The Brinell hardness values exhibit a similar pattern to tensile strength. The control sample (25.9 BHN) increased marginally to 27.1 BHN (at 2 wt%) and 28.4 BHN (at 4 wt%) ES. At 6 wt% ES, a sharp decrease to 24.8 BHN was observed, and a significant improvement to 40.2 BHN (at 8 wt%) and 32.8 BHN (10 wt%).

The hardness-composition relationship shows a strong correlation with the trends in tensile strength, proving that the

properties are governed by the same microstructural mechanisms (Mansouri Tehrani et al., 2019). In a study on Al-Si-Mg-Ti/eggshell composites, comparable improvements in hardness were observed, with the enhancement likely due to hard intermetallic phase distribution and fine grain structure (Shamim et al., 2017).

With the peak hardness at 8 wt% ES, this likely shows the combination of optimal grain refinement and homogenous distribution of Al4Ca particles. The particles have significantly higher hardness than the aluminium matrix, increasing overall material hardness while resisting plastic deformation.

The slight decrease at 10 wt% may be an indication of porosity or particle clustering at excessive levels of reinforcement, evidenced by similar studies on particulate-reinforced aluminium composites.

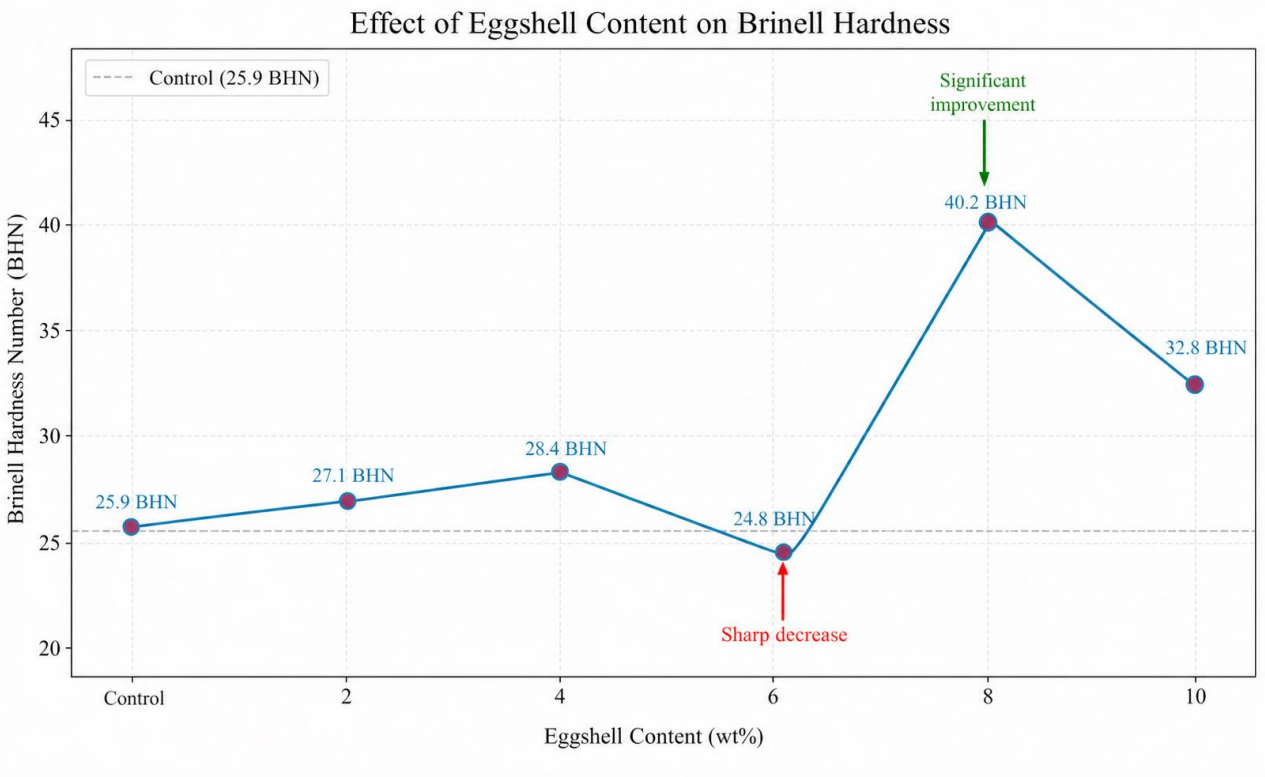

Fig. 11 Effect of eggshell (ES) particles/content on Brinell Hardness

4.3. Impact Strength

Impact strength showed an inverse linear relationship with ES particles. The control sample showed 7.03 J, and slightly increased to 7.17 J (at 2 wt% ES). However, progressive decreases were observed at subsequent additions – 6.98 J (4 wt%), 6.75 J (6 wt%), 6.30 J (8 wt%), and 6.44 J (10 wt%). This decrease in impact toughness demonstrates a key trade-off in metallurgical engineering, that an increase in strength correlates with a decrease in toughness and ductility. The brittle, hard Al4Ca intermetallic particles and refined grain structure improve strength and reduce the material's ability to absorb energy through deformation prior to its fracture (Rogachev et al., 2019).

This aligns with the research showing comparable reductions in impact strength, which explains the function of ceramic-like particles in creating crack initiation regions. During impact loading, stress concentrations at the interfaces of these matrices promote nucleation and propagation of cracks, which reduces the capacity to absorb energy (Ponnusami, Turteltaub, & van der Zwaag, 2015). The improvement at 10 wt% from 8 wt% suggests crack deflection procedures that are operative at the particles' higher densities. Meanwhile, the overall trend is inclined to decreased toughness.

4.4. Compositional Analysis

As shown in Figure 12, PIXE analysis reveals a progressive increase in calcium content with increasing ES particle additions. The control sample contained a trace amount of calcium (0.025%). This increased to 1.35%, 2.9%, 4.8%, 7.13%, and 7.09% for respective portions of 2, 4, 6, 8, and 10 wt% ES. The decrease in calcium enrichment from 7.13% to 7.09% at the highest addition is likely attributed to calcium volatilization or casting defects during processing.

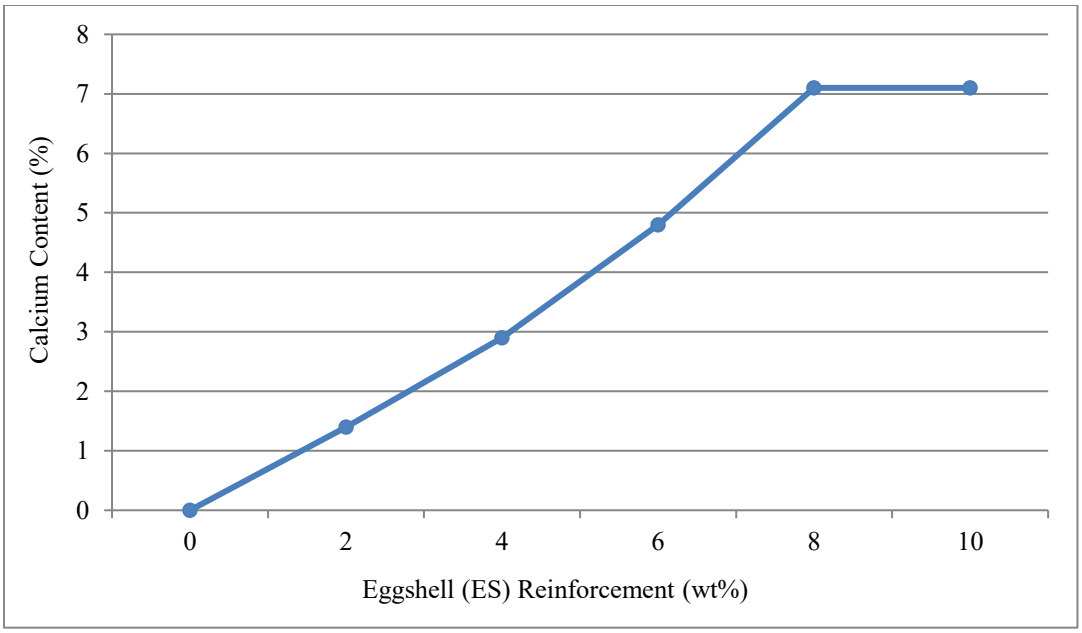

Fig. 12 PIXE analysis showing the effect of eggshell reinforcement on calcium enrichment

The data on calcium concentration confirms that ES are effective calcium sources for alloying Aluminium. The relationship between ES addition and calcium content is approximately linear (up to 8 wt%), validating the processing methodology. Other elements, including Mg, Fe, Si, Mn, and Cu, are relatively stable across compositions, indicating that calcium additions produce major metallurgical effects.

Phase equilibrium studies indicate that calcium concentrations that exceed 6-7 wt% in aluminium promote the formation of Al4Ca over other intermetallics (Naumova et al., 2019). This concentration corresponds with the shift from property degradation to improvement, and supports the hypothesis that the formation of Al4Ca is essential for improving the mechanical property of the material.

4.5. Microstructural Analysis

Optical microscopy presented an evolution of the microstructure in various compositions. The control sample (0 wt%) and low additions (2-6 wt%) showed irregular and coarse-grained structures, with the grain sizes ranging between 80 and 150 µm. On the contrary, samples with 8 wt% and 10 wt% ES revealed equiaxed and refined grain structures with sizes 30-50 µm [See Figure 6].

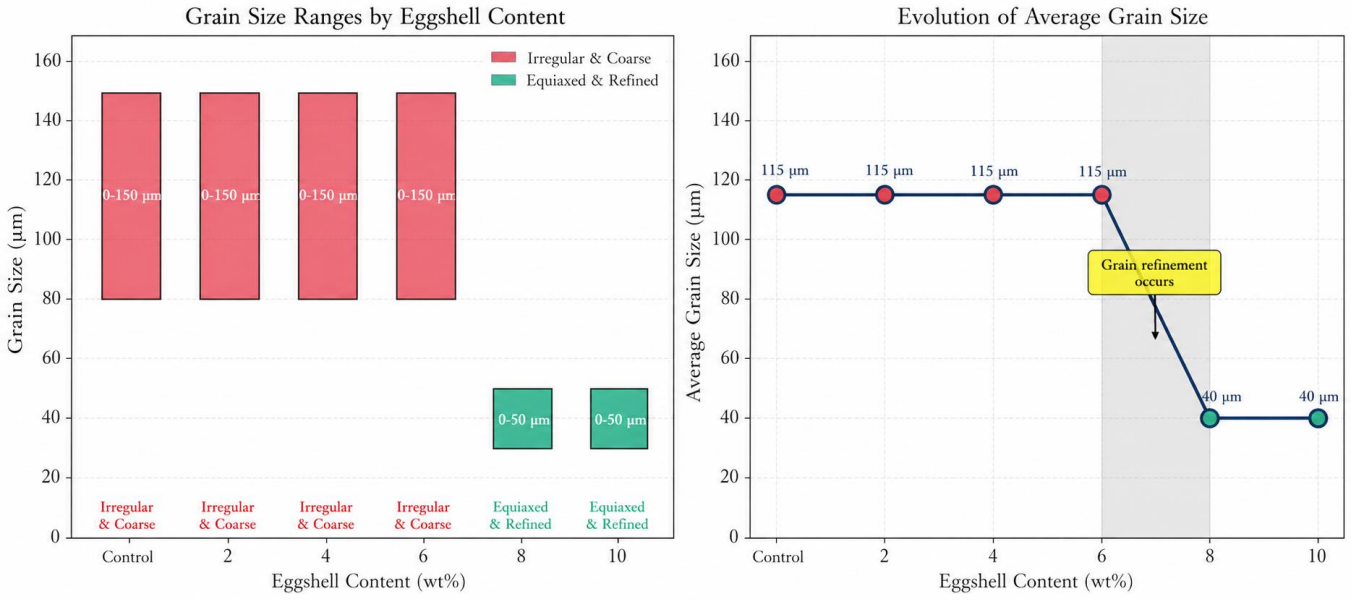

Fig. 13 Microstructural analysis using optical microscopy

The findings on grain refinement at higher Ca concentrations support established solidification theory in the literature. StJohn et al. (2015) explained that constitutional supercooling must precede the solidification front and heterogeneous nucleation sites for effective grain refinement. These achievements are achieved by calcium, with limited solubility in aluminium facilitating significant constitutional supercooling (Rohatgi, Tiwari, & Sharma, 2015).

Moving from columnar to equiaxed grain structures was observed at 6-8 wt% ES, which coincides with the improvements in mechanical properties. Current research on grain refinement procedures explains that equiaxed grains are more likely to distribute stress uniformly than columnar types, and thus, reduce stress concentrations while improving mechanical properties (Liu et al., 2019). Moreover, an increase in the boundary area of the grain, especially in fine-grained materials, provides extra barriers to dislocation motion, which explains the improved strength and hardness (Balasubramanian & Langdon, 2016).

Fine intermetallic particles distributed in the matrix were checked in high-magnification micrographs. At 8 wt% and 10 wt% ES samples [*See Figures 7.5 and 7.6]*, the particles, presumably Al4Ca due to composition, were identified as discrete and uniform particles, instead of continuous networks. Hence, effective processing and distribution are required to optimize strengthening effects and minimize embrittlement that would lead to continuous brittle phases (Jiao, Luan, & Liu, 2016; Xu et al., 2020).

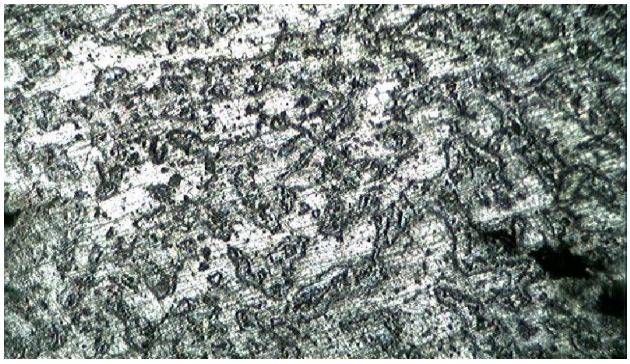

Fig. 14.1 Micrograph of Control Sample (X100)

Fig. 14.2. Micrograph of 2 wt% Sample (X100)

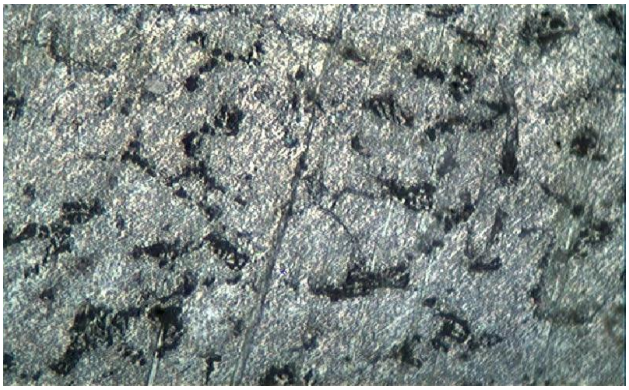

Fig. 14.3. Micrograph of 4 wt% Sample (X100)

Fig. 14.4 Micrograph of 6 wt% sample (X100)

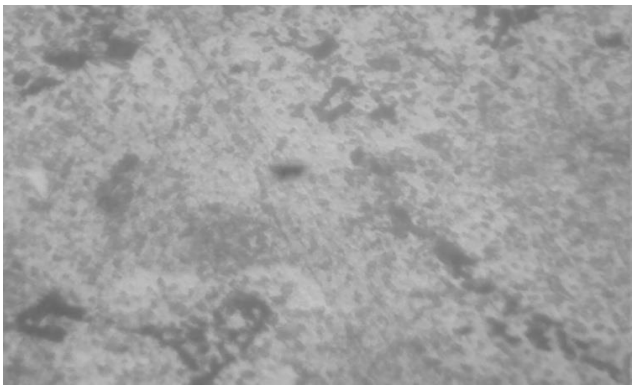

Fig. 14.5. Micrograph of 8 wt% sample (X100)

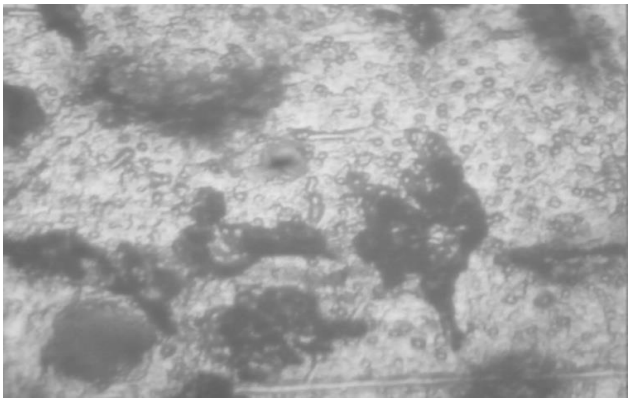

Fig. 14.6. Micrograph of 10 wt% sample (X100)

5. Conclusion and Recommendations

5.1. Conclusion

This research successfully demonstrated the use of eggshell particles as a suitable reinforcement material for recycled aluminium beverage cans. Key findings showed that recycled beverage cans contain up to 90.5% aluminium, and eggshells comprise 95% calcium carbonate. Hence, they are suitable sources of calcium for aluminium alloying. Eggshell additions below 6 wt% were detrimental to hardness and tensile strength properties, due to insufficient calcium for effective refinement of the grain and potential defect introduction.

Major property enhancements were seen at 8 wt% and 10 wt% ES additions, as tensile strength increased by 23% and hardness (by 55%) compared to other types. The study reiterated that these improvements were due to the formation of Al_4Ca intermetallic compound, acting as a primary grain refiner and strengthening agent. Increasing eggshell content led to a decrease in impact strength, which is a classical strength-toughness trade-off. At the highest reinforcement level, the maximum reduction seen was 10%.

The microstructural analysis confirmed grain refinement at 8 wt% and 10 wt%, where grain size reduced from 80-150 µm to 30-50 µm, respectively. This validated the grain refinement technique. Overall, the research establishes that ES-reinforced recycled aluminium with 8-10 wt% ES content helps to balance hardness and strength, making it suitable for applications that prioritize high surface hardness and tensile strength over impact toughness. This approach also addresses waste valorization and material performance improvement, complementing and supporting circular economy principles.

5.2. Recommendations

Based on the findings and limitations of the study, the following are recommended for future research:

1. Process optimization: Heat treatment strategies, including solution treatment and aging, should be investigated to further enhance mechanical properties. In recent literature, experts have proven that controlled aging can foster precipitation strengthening capabilities in calcium-based aluminium alloys.
2. Particle size effects: Systematic studies must be performed on the influence of eggshell particle size (within 50 – 500 µm) to identify the optimal size for maximum enhancement of its properties. For example, finer particles may yield better grain refinement, but stand the risk of agglomeration.
3. Corrosion Studies: Future research should focus on evaluating the corrosion resistance of ES-reinforced composites in various environments, especially relevant for beverage can applications involving contact with acidic beverages.
4. Hybrid Reinforcement: Combinations of ES with other bio-derived or synthetic reinforcements, including coconut shell, rice husk ash, and SiC, should be explored to balance toughness and strength. The impact strength limitation observed in the study can be addressed through hybrid composites.
5. Advanced characterization: X-Ray Diffraction (XRD) and Transmission Electron Microscopy (TEM) should be employed to identify intermetallic phases alongside their crystallographic relationships with the matrix, which confirms the Al4Ca hypothesis.

References

[1] S. Abdul, "*Investigations on Flow Characteristics and Particulate Distributions in Gyro casting of Metal Matrix Composites*," Doctoral Dissertation, 2019. [Google Scholar]

[2] E. Adabifiroozjaei, "*Interaction of BaAl2Si2O8 and CaAl2Si2O8 with Al Alloys at Different Temperatures*," Doctoral Dissertation, 2017. [Google Scholar]

[3] J.O. Agunsoye et al., "Recycled Aluminum Cans/Eggshell Composites: Evaluation of Mechanical and Wear Resistance Properties," *Tribology in Industry*, vol. 37, no. 1, pp. 107-116, 2015. [Google Scholar]

[4] Y. Ahmad, Oxidation of Graphite and Metallurgical Coke: A Numerical Study with an Experimental Approach, 2016. [Google Scholar]

[5] Darem Ahmad et al., "Hydrophilic and Hydrophobic Materials and their Applications," *Energy Sources, Part A: Recovery, Utilization, and Environmental Effects*, vol. 40, no. 22, pp. 2686-2725, 2018. [CrossRef] [Google Scholar] [Publisher Link]

[6] Ain U. Md Shah et al., "A Review on the Tensile Properties of Bamboo Fiber Reinforced Polymer Composites," *BioResources*, vol. 11, no. 4, pp. 10654-10676, 2016. [Google Scholar] [Publisher Link]

[7] Torgom Akopyan, Nikolay Belov, and Evgenia Naumova, *Calcium-Containing Aluminum Alloys*, 1st ed., Encyclopedia of Aluminum and Its Alloys, Two-Volume Set, pp. 192-206, 2018. [CrossRef] [Google Scholar] [Publisher Link]

[8] A.M. Rajesh et al., "Material Characterization of SiC and Al_2O_3–Reinforced Hybrid Aluminum Metal Matrix Composites on Wear Behavior," *Advanced Composites Letters*, vol. 28, 2019. [CrossRef] [Google Scholar] [Publisher Link]

[9] Ronald W. Armstrong et al., "Hall–Petch Relationship in Aluminum and Aluminum Alloys," *Encyclopedia of Aluminum and Its Alloys*, Two-Volume Set, CRC Press, pp. 1104-1122, 2018. [Google Scholar] [Publisher Link]

[10] S. Arunkumar et al., "Optimization of Wear Behaviour of Al7075 Hybrid Metal Matrix Composites using Taguchi Approach," *Materials Today: Proceedings*, vol. 33, pp. 570-577, 2020. [CrossRef] [Google Scholar] [Publisher Link]

[11] Eleni C. Arvaniti et al., "Determination of Particle Size, Surface Area, and Shape of Supplementary Cementitious Materials by Different Techniques," *Materials and Structures*, vol. 48, no. 11, pp. 3687-3701, 2015. [CrossRef] [Google Scholar] [Publisher Link]

[12] N. Balasubramanian, and Terence G. Langdon, "The Strength–Grain Size Relationship in Ultrafine-Grained Metals," *Metallurgical and Materials Transactions A*, vol. 47, no. 12, pp. 5827-5838, 2016. [CrossRef] [Google Scholar] [Publisher Link]

[13] Faranak Barandehfard et al., "Improving Corrosion Resistance of Aluminosilicate Refractories Towards Molten Al-Mg Alloy Using Non-Wetting Additives: A Short Review," *Materials*, vol. 13, no. 18, pp. 1-28, 2020. [CrossRef] [Google Scholar] [Publisher Link]

[14] Matthew R. Barnett, Huan Wang, and Tingting Guo, "An Orowan Precipitate Strengthening Equation for Mechanical Twinning in Mg," *International Journal of Plasticity*, vol. 112, pp. 108-122, 2019. [CrossRef] [Google Scholar] [Publisher Link]

[15] V.E. Bazhenov, and M.A. Maguraz, "Effects of Si and Cu Contents on Grain Size of Al–Si–Cu Alloys," *Materials Science and Technology*, vol. 34, no. 11, pp. 1287-1294, 2018. [CrossRef] [Google Scholar] [Publisher Link]

[16] Bello Sefiu Adekunle, "*Development and Characterisation of Epoxy-Alumininum-Coconut Shell Particulate Hybrid Nanocomposite for Automobile Applications*," Doctoral Dissertation, University of Lagos, Nigeria, 2017. [CrossRef] [Google Scholar] [Publisher Link]

[17] Nikolay Aleksandrovich Belov, Evgenia Alexandrovna Naumova, and Torgom Karoevich Akopyan, "Effect of Calcium on Structure, Phase Composition and Hardening of Al-Zn-Mg Alloys Containing up to 12wt.% Zn," *Materials Research*, vol. 18, no. 6, pp. 1384-1391, 2015. [CrossRef] [Google Scholar] [Publisher Link]

[18] Himadri Borah, and Upakul Dutta, "Trends in Beverage Packaging," *Trends in Beverage Packaging*, vol. 16, pp. 1-19, 2019. [CrossRef] [Google Scholar] [Publisher Link]

[19] Viktoriya Boyko, "*Characterization of the Structure and Precipitation Process in Al-Mg-Si and Al-Mg-Ge Casting Alloys*," Doctoral Dissertation, Technische Universität, 2015. [Google Scholar] [Publisher Link]

[20] Leslie Brooks et al., "Ferrous and Non-Ferrous Recycling: Challenges and Potential Technology Solutions," *Waste Management*, vol. 85, pp. 519-528, 2019. [CrossRef] [Google Scholar] [Publisher Link]

[21] Stefano Capuzzi, and Giulio Timelli, "Preparation and Melting of Scrap in Aluminum Recycling: A Review," *Metals*, vol. 8, no. 4, pp. 1-24, 2018. [CrossRef] [Google Scholar] [Publisher Link]

[22] Stefanie Chan et al., "SDG 12: Responsible Consumption and Production, A Review of Research Needs," Technical Annex to the Formas Report Forskning för Agenda, 2030. [Google Scholar] [Publisher Link]

[23] Atul H. Chokshi, "Grain Boundary Processes in Strengthening, Weakening, and Superplasticity," *Advanced Engineering Materials*, vol. 22, no. 1, 2020. [CrossRef] [Google Scholar] [Publisher Link]

[24] James Michael Taylor Davies, "*Effect of Titanium Diboride Particle Size on Al-Alloy Properties*," Doctoral Dissertation, University of Birmingham, 2017. [Google Scholar] [Publisher Link]

[25] Vicky Vi Thuy Doan-Nguyen, *Form and Function: X-Ray Scattering and Spectroscopy of Transition Metal-Based Nanoparticles*, University of Pennsylvania, 2015. [Google Scholar] [Publisher Link]

[26] Jennifer R. Dodson et al., "Bio-Derived Materials as a Green Route for Precious & Critical Metal Recovery and Re-Use," *Green Chemistry*, vol. 17, no. 4, pp. 1951-1965, 2015. [CrossRef] [Google Scholar] [Publisher Link]

[27] Mobolaji Dudubo, "*The Reverse Logistics of Beverage Containers-(A Case Study of Lagos, Nigeria)*," Master's Theses, 2017. [Google Scholar] [Publisher Link]

[28] Shashi Prakash Dwivedi, Satpal Sharma, and Raghvendra Kumar Mishra, "A Comparative Study of Waste Eggshells, $CaCO_3$, and SiC-Reinforced AA2014 Green Metal Matrix Composites," *Journal of Composite Materials*, vol. 51, no. 17, pp. 2407-2421, 2017. [CrossRef] [Google Scholar] [Publisher Link]

[29] S.K. Dwiwedi et al., "Eggshell-Reinforced Al6061 Matrix Composites," 2018. [Google Scholar]

[30] Williams S. Ebhota, and Tien-Chien Jen, "Mechanical Properties of Al-Si-X Alloys," *Intermetallic Compounds: Formation and Applications*, 2018. [Google Scholar]

[31] Reihaneh Etemadi et al., "On Porosity Formation in Metal Matrix Composites Made with Dual-Scale Fiber Reinforcements using Pressure Infiltration Process," *Metallurgical and Materials Transactions A*, vol. 46, no. 5, pp. 2119-2133, 2015. [CrossRef] [Google Scholar] [Publisher Link]

[32] Z. Fan et al., "Grain Refining Mechanism in the Al/Al–Ti–B System," *Acta Materialia*, vol. 84, pp. 292-304, 2015. [CrossRef] [Google Scholar] [Publisher Link]

[33] Wanlin Gao et al., "Industrial Carbon Dioxide Capture and Utilization: State of the Art and Future Challenges," *Chemical Society Reviews*, vol. 49, no. 23, pp. 8584-8686, 2020. [CrossRef] [Google Scholar] [Publisher Link]

[34] Pablo Garcia-Chevesich et al., "Inexpensive Organic Materials and their Applications towards Heavy Metal Attenuation in Waters from Southern Peru," *Water*, vol. 12, no. 10, pp. 1-34, 2020. [CrossRef] [Google Scholar] [Publisher Link]

[35] Meenu Gautam, Bhanu Pandey, and Madhoolika Agrawal, "Carbon Footprint of Aluminum Production: Emissions and Mitigation," *Environmental carbon footprints*, pp. 197-228, 2018. [CrossRef] [Google Scholar] [Publisher Link]

[36] Lindsay Greer, "Control of Grain Size in Solidification," *Solidification and Casting*, CRC Press, pp. 199-247, 2016. [Google Scholar] [Publisher Link]

[37] Ren-Guo Guan, and Di Tie, "A Review on Grain Refinement of Aluminum Alloys: Progresses, Challenges and Prospects," *Acta Metallurgica Sinica*, vol. 30, no. 5, pp. 409-432, 2017. [CrossRef] [Google Scholar] [Publisher Link]

[38] A. Hauksdóttir, "*Geothermal Energy: Silica Precipitation and Utilization*," Doctoral Dissertation, 2016. [Google Scholar]

[39] Mohammed T. Hayajneh, Mohammed A. Almomani, and Mu'ayyad M. Al-Shrida, "Effects of Waste Eggshells Addition on Microstructures, Mechanical and Tribological Properties of Green Metal Matrix Composite," *Science and Engineering of Composite Materials*, vol. 26, no. 1, pp. 423-434, 2019. [CrossRef] [Google Scholar] [Publisher Link]

[40] Javier Hidalgo, and Maria Jesus Santofimia, "Effect of Prior Austenite Grain Size Refinement by Thermal Cycling on the Microstructural Features of as-Quenched Lath Martensite," *Metallurgical and Materials Transactions A*, vol. 47, no. 11, pp. 5288-5301, 2016. [CrossRef] [Google Scholar] [Publisher Link]

[41] S. Hossain, and P.K. Roy, "Sustainable Ceramics Derived From Solid Wastes: A Review," *Journal of Asian Ceramic Societies*, vol. 8, no. 4, pp. 984-1009, 2020. [CrossRef] [Google Scholar] [Publisher Link]

[42] Zhong-tao Jiang et al., "Effect of Al_2Ca Intermetallic Compound Addition on Grain Refinement of AZ31 Magnesium Alloy," *Transactions of Nonferrous Metals Society of China*, vol. 26, no. 5, pp. 1284-1293, 2016. [CrossRef] [Google Scholar] [Publisher Link]

[43] Z.B. Jiao, J.H. Luan, and C.T. Liu, "Strategies for Improving Ductility of Ordered Intermetallics," *Progress in Natural Science: Materials International*, vol. 26, no. 1, pp. 1-12, 2016. [CrossRef] [Google Scholar] [Publisher Link]

[44] A. Juniarsih, S. Oediyani, and A.P. Zain, "The Effect of Flux's Towards Mg Reduction from Aluminium Beverage Cans," *IOP Conference Series: Materials Science and Engineering*, vol. 478, no. 1, pp. 1-, 2019. [CrossRef] [Google Scholar] [Publisher Link]

[45] Bhaskar Chandra Kandpal, Jatinder Kumar, and Hari Singh, "Manufacturing and Technological Challenges in Stir Casting of Metal Matrix Composites: A Review," *Materials Today: Proceedings*, vol. 5, no. 1, pp. 5-10, 2018. [CrossRef] [Google Scholar] [Publisher Link]

[46] Leiv Kolbeinsen, "The Beginning and the End of the Aluminium Value Chain," *Matériaux & Techniques*, vol. 108, no. 5-6, pp. 1-22, 2020. [CrossRef] [Google Scholar] [Publisher Link]

[47] V. Mahesh Kumar, and C.V. Venkatesh, "A Comprehensive Review on Material Selection, Processing, Characterization and Applications of Aluminium Metal Matrix Composites," *Materials Research Express*, vol. 6, no. 7, 2019. [CrossRef] [Google Scholar] [Publisher Link]

[48] Jiehua Li et al., "Heterogeneous Nucleation of Al on AlB_2 in Al-7Si Alloy," *Materials Characterization*, vol. 128, pp. 7-13, 2017. [CrossRef] [Google Scholar] [Publisher Link]

[49] Jia Li et al., "Fine-Grain-Embedded Dislocation-Cell Structures for High Strength and Ductility in Additively Manufactured Steels," *Materials Science and Engineering: A*, vol. 790, 2020. [CrossRef] [Google Scholar] [Publisher Link]

[50] Pengwei Liu et al., "Insight into the Mechanisms of Columnar to Equiaxed Grain Transition during Metallic Additive Manufacturing," *Additive Manufacturing*, vol. 26, pp. 22-29, 2019. [CrossRef] [Google Scholar] [Publisher Link]

[51] Hong Liu et al., "Phase-Field Simulation of Orowan Strengthening by Coherent Precipitate Plates in an Aluminum Alloy," *Metallurgical and Materials Transactions A*, vol. 46, no. 7, pp. 3287-3301, 2015. [CrossRef] [Google Scholar] [Publisher Link]

[52] Aria Mansouri Tehrani et al., "Atomic Substitution to Balance Hardness, Ductility, and Sustainability in Molybdenum Tungsten Borocarbide," *Chemistry of Materials*, vol. 31, no. 18, pp. 7696-7703, 2019. [CrossRef] [Google Scholar] [Publisher Link]

[53] Ana C. Marques et al., "Review on Adhesives and Surface Treatments for Structural Applications: Recent Developments on Sustainability and Implementation for Metal and Composite Substrates," *Materials*, vol. 13, no. 24, pp. 1-43, 2020. [CrossRef] [Google Scholar] [Publisher Link]

[54] V. Mohanavel et al., "Microstructural and Tribological Characteristics of AA6351/Si_3N_4 Composites Manufactured by Stir Casting," *Journal of Materials Research and Technology*, vol. 9, no. 6, pp. 14662-14672, 2020. [CrossRef] [Google Scholar] [Publisher Link]

[55] J.A. Monroe et al., "Tailored Thermal Expansion Alloys," *Acta Materialia*, vol. 102, pp. 333-341, 2016. [CrossRef] [Google Scholar] [Publisher Link]

[56] Innocent Mutsakatira, "*The Effect of the Surface Condition of Aluminium Ingot (AA3003) during Roll Bonding with Clad Aluminium Alloy (AA4045) to form an Aluminium Brazing Material*," Master Thesis, 2020. [Google Scholar] [Publisher Link]

[57] E.A. Naumova et al., "Effect of Ca and Zn Alloying on the Structure and Properties of Al - 2.5% Mg alloy," *Non-Ferrous Metals*, vol. 46, no. 1, pp. 22-27, 2019. [Google Scholar] [Publisher Link]

[58] Monia Niero, and Stig Irving Olsen, "Circular Economy: To Be or Not to Be in a Closed Product Loop? A Life Cycle Assessment of Aluminium Cans with Inclusion of Alloying Elements," *Resources, Conservation and Recycling*, vol. 114, pp. 18-31, 2016. [CrossRef] [Google Scholar] [Publisher Link]

[59] Gururaj Parande et al., "A Study on the Effect of Low-Cost Eggshell Reinforcement on the Immersion, Damping and Mechanical Properties of Magnesium–Zinc Alloy," *Composites Part B: Engineering*, vol. 182, 2020. [CrossRef] [Google Scholar] [Publisher Link]

[60] Sathiskumar A. Ponnusami, Sergio Turteltaub, and Sybrand van der Zwaag, "Cohesive-Zone Modelling of Crack Nucleation and Propagation in Particulate Composites," *Engineering Fracture Mechanics*, vol. 149, pp. 170-190, 2015. [CrossRef] [Google Scholar] [Publisher Link]

[61] Margarida J. Quina, Micaela A.R. Soares, and Rosa Quinta-Ferreira, "Applications of Industrial Eggshell as a Valuable Anthropogenic Resource," *Resources, Conservation and Recycling*, vol. 123, pp. 176-186, 2017. [CrossRef] [Google Scholar] [Publisher Link]

[62] Felipe Robles Poblete, and Yong Zhu, "Interfacial Shear Stress Transfer at Nanowire-Polymer Interfaces with Van Der Waals Interactions and Chemical Bonding," *Journal of the Mechanics and Physics of Solids*, vol. 127, pp. 191-207, 2019. [CrossRef] [Google Scholar] [Publisher Link]

[63] Maria Cristina Santos Ribeiro et al., "Recycling Approach towards Sustainability Advance of Composite Materials' Industry," *Recycling*, vol. 1, no. 1, pp. 178-193, 2016. [CrossRef] [Google Scholar] [Publisher Link]

[64] S.O. Rogachev et al., "Structure and Mechanical Properties of Al–Ca Alloys Processed by Severe Plastic Deformation," *Materials Science and Engineering: A*, vol. 767, 2019. [CrossRef] [Google Scholar] [Publisher Link]

[65] Shivangi Rohatgi et al., "Role of Undercooling and Effect of Solute Particles on Grain Refinement of Aluminium Alloys," *Indian Foundry Journal*, vol. 62, pp. 31-37, 2015. [Google Scholar] [Publisher Link]

[66] Anna Sapota, "Aluminium Cans as a Source of End User's Scrap," *Aluminium International Today*, vol. 32, no. 3, pp. 20-21, 2019. [Google Scholar]

[67] Xavier Sauvage et al., "Understanding the Role of Ca Segregation on Thermal Stability, Electrical Resistivity and Mechanical Strength of Nanostructured Aluminum," *Materials Science and Engineering: A*, vol. 798, 2020. [CrossRef] [Google Scholar] [Publisher Link]

[68] Shahrukh Shamim et al., "Microstructures and Mechanical Properties of Al-Si-Mg-Ti/Egg Shell Particulate Composites," *Materials Today: Proceedings*, vol. 4, no. 2, pp. 2887-2892, 2017. [CrossRef] [Google Scholar] [Publisher Link]

[69] A. Shashikala, "Aluminium an Important Metal for India's Sustainable and Circular Economy," *Journal of Energy and Environmental Sustainability*, vol. 10, pp. 6-16, 2020. [Google Scholar] [Publisher Link]

[70] Zoban Veer Singh, "*Design and Evaluation of New Mixed-Matrix Membranes for CO_2/CH_4 Separations,*" Doctoral Dissertation, University of Colorado Boulder, 2017. [Google Scholar] [Publisher Link]

[71] Vi Kie Soo et al., "Sustainable Aluminium Recycling of End-of-Life Products: A Joining Techniques Perspective," *Journal of Cleaner Production*, vol. 178, pp. 119-132, 2018. [CrossRef] [Google Scholar] [Publisher Link]

[72] D.H. John et al., "The Contribution of Constitutional Supercooling to Nucleation and Grain Formation," *Metallurgical and Materials Transactions A*, vol. 46, no. 11, pp. 4868-4885, 2015. [CrossRef] [Google Scholar] [Publisher Link]

[73] Philippe Maurice Stotz et al., "Environmental Screening of Novel Technologies to Increase Material Circularity: A Case Study on Aluminium Cans," *Resources, Conservation and Recycling*, vol. 127, pp. 96-106, 2017. [CrossRef] [Google Scholar] [Publisher Link]

[74] Patrick T. Summers et al., "Overview of Aluminum Alloy Mechanical Properties During and After Fires," *Fire Science Reviews*, vol. 4, no. 1, pp. 1-36, 2015. [CrossRef] [Google Scholar] [Publisher Link]

[75] Wenwen Sun et al., "Precipitation Strengthening of Aluminum Alloys by Room-Temperature Cyclic Plasticity," *Science*, vol. 363, no. 6430, pp. 972-975, 2019. [CrossRef] [Google Scholar] [Publisher Link]

[76] D.H. Thompson et al., "Interstitial-Mediated Dislocation Climb and the Weakening of Particle-Reinforced Alloys Under Irradiation," *Physical Review Materials*, vol. 2, no. 8, 2018. [CrossRef] [Google Scholar] [Publisher Link]

[77] Thijs van Westen, and Robert D. Groot, "Effect of Temperature Cycling on Ostwald Ripening," *Crystal Growth & Design*, vol. 18, no. 9, pp. 4952-4962, 2018. [CrossRef] [Google Scholar] [Publisher Link]

[78] Marium Waheed et al., "Channelling Eggshell Waste to Valuable and Utilizable Products: A Comprehensive Review," *Trends in Food Science & Technology*, vol. 106, pp. 78-90, 2020. [CrossRef] [Google Scholar] [Publisher Link]

[79] Yachao Wang, and Jing Shi, "Engulfment and Distribution of Second-Phase Nanoparticle during Dendrite Solidification of an Al–Si Binary Alloy: A Simulation Study," *Applied Physics A*, vol. 125, no. 6, 2019. [CrossRef] [Google Scholar] [Publisher Link]

[80] Omar Bashir Wani et al., "Understanding the Wettability of Calcite ($CaCO_3$) Using Higher Spatial Resolution," *Energy & Fuels*, vol. 32, no. 10, pp. 10344-10353, 2018. [CrossRef] [Google Scholar] [Publisher Link]

[81] Chuandong Wu et al., "Influence of Particle Size and Spatial Distribution of B_4C Reinforcement on the Microstructure and Mechanical Behavior of Precipitation Strengthened Al Alloy Matrix Composites," *Materials Science and Engineering: A*, vol. 675, pp. 421-430, 2016. [CrossRef] [Google Scholar] [Publisher Link]

[82] Jinghao Xu et al., "On the Strengthening and Embrittlement Mechanisms of an Additively Manufactured Nickel-Base Superalloy," *Materialia*, vol. 10, pp. 1-13, 2020. [CrossRef] [Google Scholar] [Publisher Link]

[83] Xiaomin Yuan et al., "Effects of Particle Size and Distribution of the Sizing Agent on Carbon Fiber/Epoxy Composites Interfacial Adhesion," *Polymer Composites*, vol. 39, no. S4, pp. E2036-E2045, 2018. [CrossRef] [Google Scholar] [Publisher Link]

[84] Yu Zhang et al., "The Influences of Al Content on the Microstructure and Mechanical Properties of As-Cast Mg-6Zn Magnesium Alloys," *Materials Science and Engineering: A*, vol. 686, pp. 93-101, 2017. [CrossRef] [Google Scholar] [Publisher Link]